UNIVERSITY OF TWENTE.

Project Title:	Toward next-generation 3D printed materials for space applications: hierarchical nanoporous structures with engineered macro-architectures		
Project Number	4000135470	Start date	End date
		01-09-2021	30-04-2023
Period	M1-M18		
Author(s)	Dr. A. (Ahmad) Zafari Dr. D. (Davoud) Jafari Dr. A. (Antoni) Forner Cuenca Dr. S. (Salome) Sanchez Dr. K (Kiran) Bhatia		

Document Type	Name	Description	Milestone	WP no.	Delivery date (in month)
R	D0.4	Executive Summary	End of WP6	0	M18

	Prepared & verified	Approved	Authorized
Name	D. Jafari		
Date	01-05-2023		
Signature			

Revision Index		
Issue	Prepared/Date	Remarks
6.0	D. Jafari 01-05-2022	First version

UNIVERSITY OF TWENTE.

Summary

This document is a short summary of the abovementioned project, providing an overview of the objectives, methodology and main findings. The first section is a brief introduction into the application of porous electrodes in fuel cells, gaps in the literature, and the aims of the present work. Afterwards, a general picture of the approach taken (i.e., methods) followed by the main achievements will be presented. The reports will be ended with concluding remarks and suggestions for future work.

1. Objectives and scope of the project

The main goal of this project was to fabricate porous electrodes used in fuel cells. Figs.1a and b schematically show different parts in a fuel cell and a porous electrode, respectively. As seen, a porous electrode consists of a catalyst layer (CL), microporous layer (MPL) and gas diffusion layer (GDL). GDLs are conventionally made of carbon paper or cloth. However, there are several drawbacks, including degregation in alkalin media, deformation, and consequently, closure of pores under compression, and randomness of pore charactristics (e.g., pore size and distribution). As an alternative, metallic GDLs with much greater mechanical strengths have recently been introduced for alkalin environements. Porous metallic materials are conventionally produced by powder/fiber sintering, and foaming [12-14]. However, these processes are unable to precisely control pore size, morphology, and distribution, limiting the performance of the resultant systems. Thus, there is a need for developing new material sets with specific micro/macro-structures and surface properties to enable the next-generation of electrochemical technologies.

To overcome these challenges, laser powder bed fusion (LPBF), as a common additive manufacturing (AM) method with the highest spatial resolution, was used to control the formation and characteristics of pores in Ti-6Al-4V and Inconel 718 (In718) GDLs by manipulating laser parameters and pore geometries. Following LPBF, an additional step of the electrodeposition of porous Ni catalyst was also performed to improve electrochemical efficiency. Hydrogen and oxygen evolution reactions (HER and OER) were examined in a classical three electrode cell to test the electrochemical performance of the electrodes.

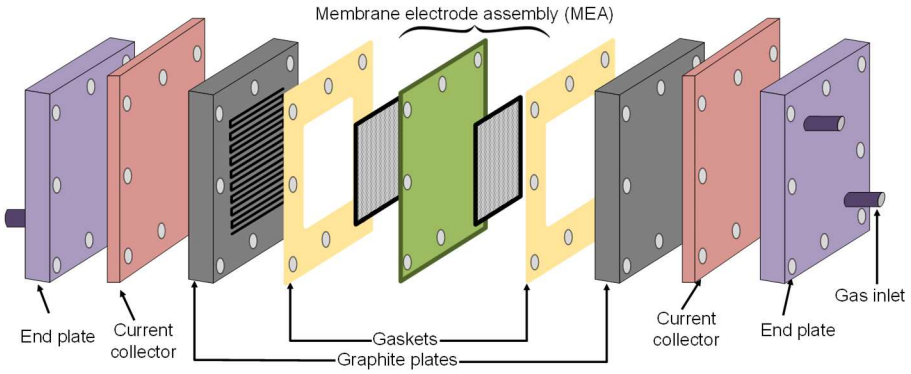

(a)

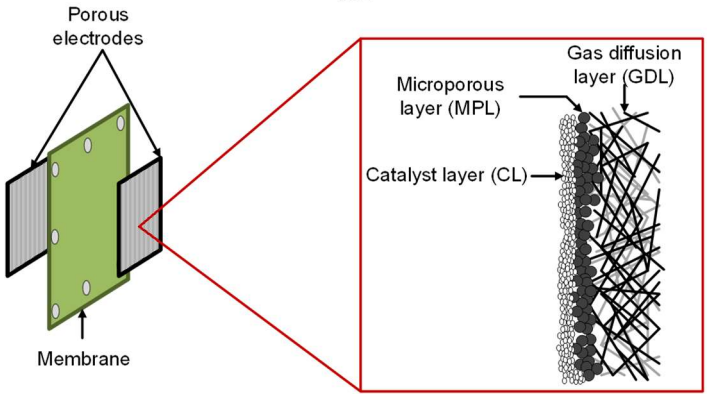

(b)

Fig. 1 Schematics of (a) the exploded view of a fuel cell, (b) a porous electrode consisting of catalyst, microporous and gas diffusion layers.

2. Achievements

The main achievements of the project are listed as follows.

- LPBF of thin walled porous Ti-6Al-4V GDLs resulted in pores of < 20 µm with the porosity of ~39-60%. Regularly spaced solid/free-space columns were also formed in a set of thin walls thanks to careful optimisation of laser parameters.
- Geometrically defined lattice structure porosity was successfully obtained in both Ti-6Al-4V and In718 electrodes.
- Electrodeposition of Ni led to the formation of pores of the order of 100 nm to 1 µm. This together with the macro-pores obtained from LPBF resulted in multimodal pores, which was one of the objectives of the project.
- Both Ti-6Al-4V and In718 electrodes exhibited good electrochemical performances. However, the main difference between them was that Ti-6Al-4V was inactive, producing no current before Ni deposition. Additionally, for OER, In718 showed the same electrochemical behaviour with and without Ni catalyst.
- Overall, the main objectives of the project, including defining pore characteristics (e.g., pore size, pore geometry and distribution), producing multimodal pores ranging from macro to nano scales, and high electrochemical efficiency by electrodeposition, were achieved by combining LPBF and electrodeposition.

3. Detailed results

3.1. Thin walled Ti-6Al-4V

Laser energy density was manipulated by changing laser power, scanning speed and duty cycle (see Fig. 2) to induce porosity in thin walls of 100-200 µm. Among the thin walls obtained, the one fabricated using a duty cycle of 87.5%, scanning speed of 1500 mm/s, and power of 100 W was identified as optimum because it had a regular structure consisting of equally spaced solid and free-space columns, as shown in Fig. 3. The exact structure could be achieved by repeating the printing process, unlike others in which pores formed randomly.

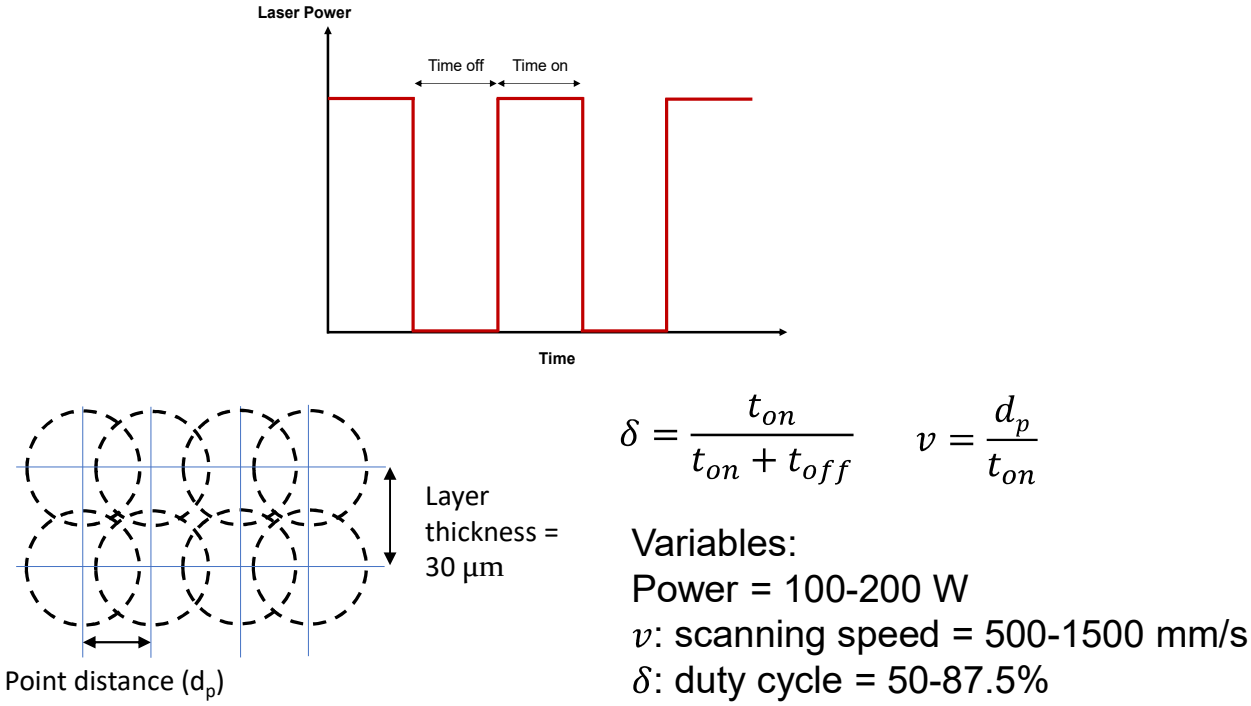

Fig. 2 Schematics of (top) variation of laser power with time for a pulsed laser, and (bottom left) laser point distance and layer thickness, and (bottom right) equations using which duty cycle and scanning speed were calculated, as well as a range of duty cycles, powers and scanning speeds used to produce thin walls.

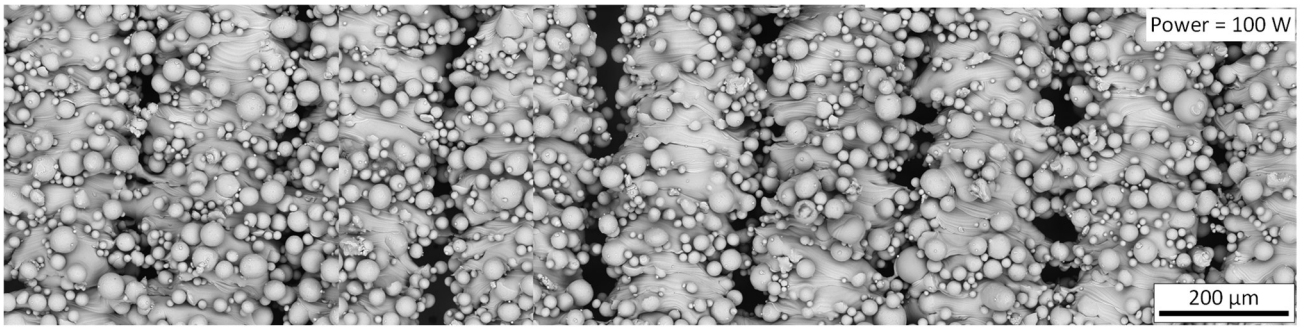

Fig. 3 SEM image of a thin wall produced using duty cycle of 87.5%, scanning speed of 1500 mm/s, and power of 100 W.

3.2. Ti-6Al-4V lattice structures

Different unit cells of body centered cubic (BCC), hexagon and octagon were used to produce porous electrodes, among which hexagon led to best electrochemical performance (results will be provided later). Fig. 4 shows SEM images of GDLs made of hexagon unit cells with the strut thicknesses of 0.15-0.35 mm. As seen, pore size, location, distribution and geometry were all well defined using the hexagon unit cells whose characteristics could digitally be defined in a CAD model.

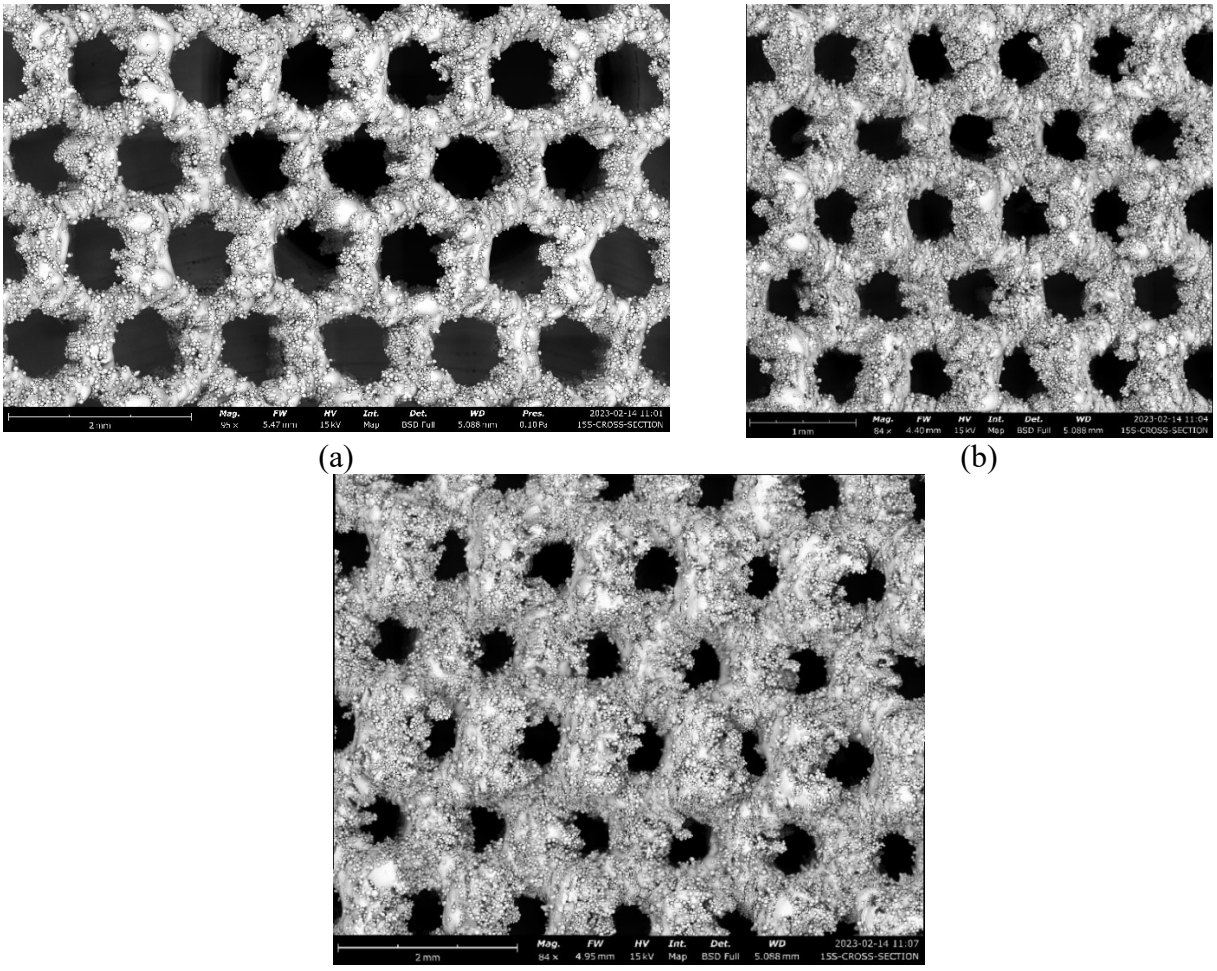

Fig. 3 SEM of cellular structures with strut sizes designed to be (a) 0.15 mm, (b) 0.25 mm and (c) 0.35 mm.

3.3. Electrodeposition of Ni

Following deposition in planar substrates, the best performing electrodeposition conditions were applied to the printed cellular Ti-6Al-4V electrode. Fig. 4a-c depicts the structural analysis of pristine Ti-6Al-4V. At higher magnifications, spherical sintered particles were observed with varying diameters. In the case of printed cellular Ti-6Al-4V, the porous network starts to form on top of these sintered spherical particles, however, the distribution of these pores are not very uniform, which could be accounted for nonuniformity of pore network in Ni coatings since the bubble break off diameter could be different for the sintered particles with varying diameters (Fig. 4d-f). The side walls of the pores have a honeycomb/cauliflower-like structure (Fig. 4d-f), resulting in pores on the meso and micro scales.

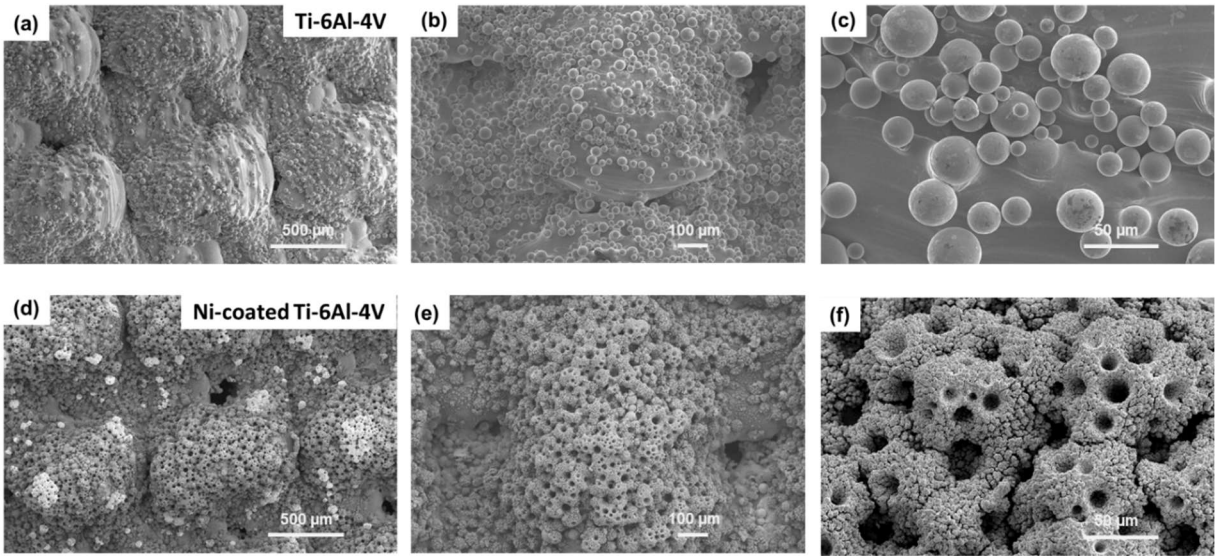

Fig. 4 SEM Micrographs of (a-c) an as-LPBF Ti-6Al-4V BCC lattice structure, and (d-f) after Ni foam deposition.

3.4. Electrochemical properties of Ti-6Al-4V electrodes

The polirisation curves for hydrogen evolution reaction (HER) and oxygen evolution reaction (OER) obtained from thin walled and cellular structured Ti-6Al-4V are shown in Figs. 5a and b, respectively. The values of 150-350 µm denote the strut thicknesses in hexagon unit cells (Fig. 3). For the HER, all of the electrodes exhibited good performance, with the best one shown by Ni-coated Ti-6Al-4V 350 µm attaining up to −410 mA cm^{-2} at iR corrected potential of ~ −0.4 V vs RHE (Fig. 5a). Similarly, the same sample showed the best performance for OER, producing a maximum current density of ~360 mA cm^{-2} at iR corrected potential of ~ 1.78 V vs RHE (Fig.5b green curve). This can be attributed to the synergy between the coating and Ti-6Al-4V 350µm facilitating the reactions when compared to other Ti-6Al-4V electrodes.

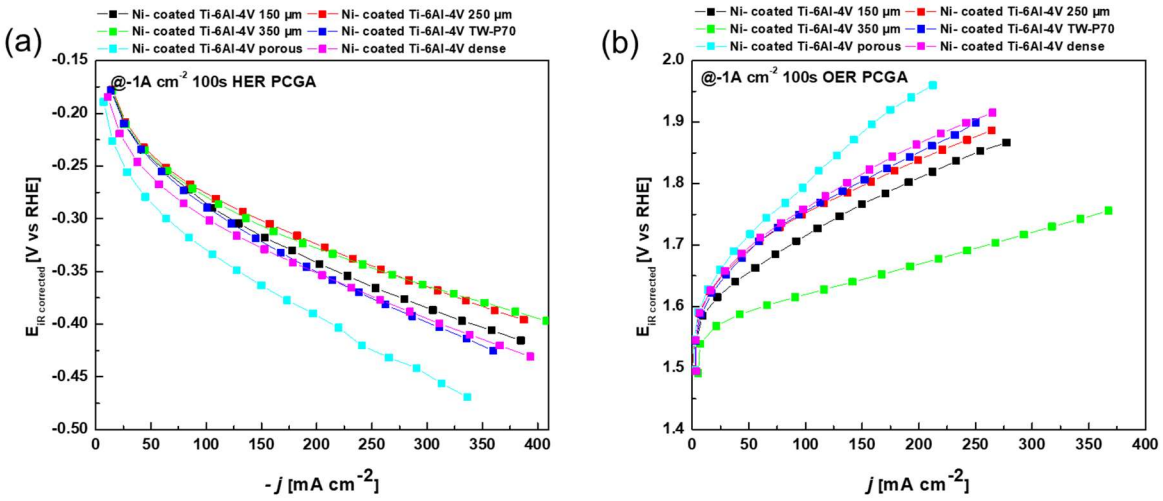

Fig. 5. Comparison of polarisation curves of Ni-coated LPBF Ti-6Al-4V alloy with different strut thicknesses (a) for OER; (b) for HER. For all the electrodes same deposition conditions and protocol was applied.

3.5. In718 lattice structures

Different designs with different unit cell and strut sizes were printed, and the design which was printed successfully with well-defined pores was selected as the optimum. More specifically, the optimum design was made of BCC unit cells of 0.5 mm and struts of 0.2 mm. The measured pore size and porosity in the LPBF-fabricated electrode were ~100 µm and > 50%, respectively. Figs. 6a and b show SEM of an as-LPBF and a cross section of the optimum electrode, respectively.

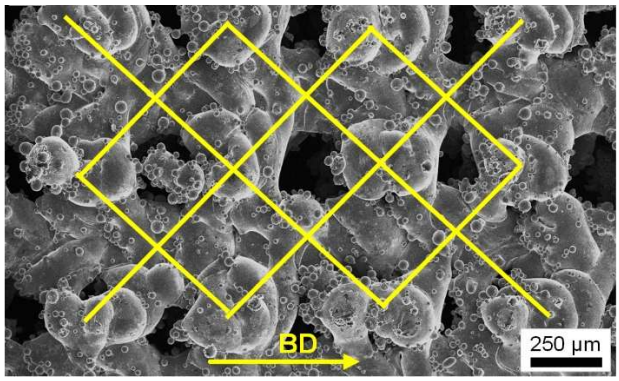

(a)

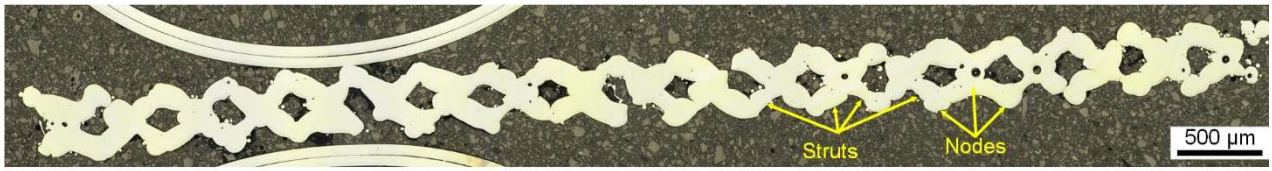

(b)

Fig. 6 Microstructure of an In718 electrode with an optimum design: (a) SEM of the as-LPBF electrode, and (b) optical microscopy of a cross section of the electrode.

3.6. Electrochemical properties of In718 lattice structures

The structure of Ni catalyst deposited on In718 electrodes was the same as that on Ti-6Al-4V ones (Fig. 4). Hence, it is not shown here. Figs. 7a and b show polarisation curves for HER and OER, respectively. For HER, a much larger maximum current density of ~ 360 mA/cm^2 at a less negative potential of ~ −0.43 V was produced in the Ni-coated specimen, as compared to 250 mA/cm^2 at ~ −0.67 V in the bare one, indicating its superior performance. For OER, however, both bare and Ni-coated electrodes similarly showed a maximum current density of ~350 mA/cm^2 at ~ 1.8 V.

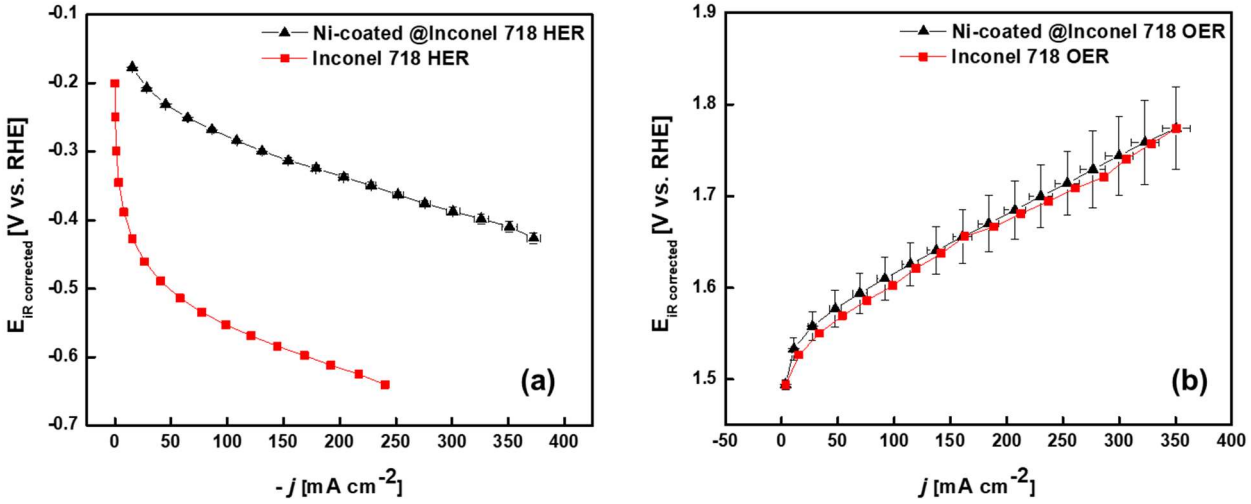

Fig. 7 Polarisation curves for (a) HER and (b) OER obtained from Ni-coated In718 (black) and as-LPBF In718 (red) electrodes.

4. Concluding discussion

The extensive experimental work on thin walled and lattice GDLs produced using LPBF led to several important discoveries.

First, in both cases of Ti-6Al-4V and In718 lattice structures, pore formation was reasonably well controlled so that geometry, location and distribution of pores could be designed using digital models. Though, the lattice-structured electrodes of ~500-700 µm in thickness were the thinnest achievable. Any thinner electrodes were either fractured during printing or turned out as solid walls. However, conventional electrodes are much thinner. One solution was to fabricate electrodes as thin as 100-200 µm by printing single laser tracks of Ti-6Al-4V on top of each other. Despite these desired thicknesses, the electrodes significantly lacked structural integrity. Nevertheless, this was still an important finding, because it indicated a promising future for LPBF to be used for manufacturing ultrathin electrodes, but a method should still be developed to increase the strengths of such thin walls. Second, the differences observed in OER results from Ti-6Al-4V and In718 electrodes, revealed that chemical compositions of GDLs could play an important role in electrochemical performance of the electrodes. More specifically, Fe in In718 could be a reason why the bare electrodes behaved the same as the Ni-coated ones, despite smaller surface area. Finally, unit cell size and design played a significant role in electrochemical performances of Ti-6Al-4V electrodes, so that those with hexagon unit cells and larger pores performed substantially better than the ones with BCC unit cells and much finer pores. Further, the strut thickness could play an important role in HER and OER data, perhaps owing to the amount of Ni catalyst deposited on the accessible surface area on the electrodes which was determined by the strut thickness. This suggests that further works can be done to find a quantitative relationship between electrochemical behavior and design parameters.